



Article

P-Bifurcation Analysis for a Fractional Damping Stochastic Nonlinear Equation with Gaussian White Noise

Yujie Tang, Yun Peng, Guitian He , Wenjie Liang and Weiting Zhang

College of Mathematics and Physics, Center for Applied Mathematics of Guangxi Minzu University, Nanning 530006, China

* Correspondence: heguitian100@163.com

Abstract: This work aims to address the P-bifurcation of a stochastic nonlinear system with fractional damping driven by Gaussian white noise. Based on a stochastic averaging method, a fractional damping stochastic nonlinear equation has been studied. Furthermore, the expressions of drift and diffusion coefficients of the Fokker–Planck equation (FPKE) have been obtained. The probability density function (PDF), the steady solution of FPKE, has also been derived. Then, PDFs of two fractional damping Morse oscillators have been obtained. One can note that the analytical results coincide with the results of numerical simulation. Importantly, stochastic P-bifurcation of a fractional damping stochastic nonlinear Morse oscillator has been further addressed and analyzed.

Keywords: stochastic averaging procedure; fractional derivative; P-bifurcation; Morse oscillator; Gaussian white noise



Citation: Tang, Y.; Peng, Y.; He, G.; Liang, W.; Zhang, W. P-Bifurcation Analysis for a Fractional Damping Stochastic Nonlinear Equation with Gaussian White Noise. *Fractal Fract.* **2023**, *7*, 408. <https://doi.org/10.3390/fractalfract7050408>

Academic Editors: Vassili Kolokoltsov and Ivanka Stamova

Received: 1 March 2023

Revised: 25 April 2023

Accepted: 16 May 2023

Published: 18 May 2023



Copyright: © 2023 by the authors. Licensee MDPI, Basel, Switzerland. This article is an open access article distributed under the terms and conditions of the Creative Commons Attribution (CC BY) license (<https://creativecommons.org/licenses/by/4.0/>).

1. Introduction and Background

Fractional calculus (FC) has proven to have a wide range of applications. As early as the days of the establishment of integral calculus, some mathematicians began to consider the significance of FC, including Fourier, Abel, Riemann and Liouville, who made many contributions to the FC theory and formed a relatively complete FC definition [1–5].

With long-term unremitting efforts, FC theory has been established to a certain extent. Unfortunately, for a long time, FC was only a pure theoretical problem in the field of mathematics. Until recent decades, many scholars were surprised to find that the fractional order model is more suitable than the integer order model in solving some problems. Since then, fractional order models have been widely used in many fields [6–11].

In the natural, engineering and social fields, there are inevitable random excitations, such as atmospheric turbulence, ocean waves, earthquakes, jet noise and fluctuations of biological groups. The stochastic dynamics of systems with fractional derivatives attract many scholars to study them. There have been some effective methods to study the equations of nonlinear dynamic systems expressed by fractional differential equations, such as stochastic averaging method [12], path integral method [13], eigenvector expansion method [14], multi-scale method [15,16], Laplace transform [17], and Fourier transform [18,19]. These methods are of great significance to the study of nonlinear dynamic systems.

Stochastic analysis draws great attention due to its application in quantum physics, statistical physics, hydrodynamics, biology, economics, and mechanics [20]. The results obtained by applying the method of stochastic averaging to random vibration problems are discussed in [21]. The response and stability for a single-degree-of-freedom stochastic system has been studied by the stochastic averaging method [22]. The analytical solution of fractional nonlinear system has been addressed in [23]. As a unique nonlinear complex phenomenon in the field of dynamic systems, stochastic bifurcation is dedicated to evaluating the qualitative change of system response when the critical parameters change within a given time interval. Therefore, the study of stochastic bifurcation is helpful to understand the current state of system response and judge its change direction or range [24].

At present, there are two kinds of research methods to analyze stochastic bifurcation: one is to determine stochastic bifurcation by studying the change of the curve shape of probability density function, which is called phenomenological bifurcation (P-bifurcation); and the second is to determine the stochastic bifurcation of the system through the variation of the maximum Lyapunov exponent sign. That is called dynamic bifurcation (D-bifurcation).

In recent decades, stochastic bifurcation has been extensively used in engineering, physics, chemistry, economics, biology and other fields, and many achievements have been made so far. In 1984, Horsthemke and Lefever [25] published the first monograph on stochastic bifurcation. Zhu [26] studied stochastic Hopf bifurcation of a quasi-nonintegrable-Hamiltonian system using the stochastic averaging method. Yang [27] addressed P-bifurcation of a fractional-order vibration energy harvester under colored noise excitation. Schenk-Hoppé [28,29] investigated Hopf bifurcation based on the theory of stochastic dynamics together with a numerical method. Using the stochastic averaging and Khasminskii's procedures, Zhu [30] investigated linear and nonlinear stochastic systems.

In the research of stochastic dynamic behavior, most of it is based on a Duffing oscillator. Based on the original van del Pol–Duffing oscillator mathematical model, this article introduces the Morse potential energy function instead of the original Duffing oscillator potential model to explore the stochastic P-bifurcation behavior of the Morse oscillator.

One knows that the Morse oscillator is widely used to describe the diatomic molecule in an electromagnetic field [31,32]. For instance, the motions of polyatomic molecules or diatomic molecules under an infrared laser environment can be modeled by the Morse oscillator [31,32]. Recently, fisher information [33] and vibrational resonance [34] of Morse oscillators have been investigated. The main difference between a Morse oscillator and harmonic oscillator is that it describes the non-bonding state, and the introduction of Morse potential energy can more accurately describe the molecular vibration.

In the present paper, based on the original mathematical model of the harmonic oscillator, the Morse potential energy function is introduced to replace the original simple harmonic oscillator potential model, and with the procedure of stochastic averaging, the approximation solution of a class fractional damping stochastic nonlinear equation governed by a general potential will be studied. Furthermore, the PDFs of two fractional damping stochastic Morse oscillators will be addressed in detail. Moreover, stochastic P-bifurcation of will also be discussed.

2. PDF for a Class Fractional Damping Stochastic Nonlinear Equation

One knows that mechanics models can be established by fractional differential equation due to viscoelastic bodies described by power-law kernels [35]. Additionally, the Hamiltonian system is often immersed in weak noise. Thus, a nonlinear conservative oscillator with small scale fractional derivative damping driven by white noise can be given by

$$\ddot{X}(t) + \varepsilon c_1 D_C^\alpha X(t) + \varepsilon c_2 h(X, \dot{X}) + g(X) = W(t), \quad 0 < \alpha < 1, \quad (1)$$

in which ε presents a small positive constant. c_1 , c_2 are two constant coefficients. $g(X)$ stands for a nonlinear continuous function of X . $h(X, \dot{X})$ denotes a continuous function of X and \dot{X} . $W(t)$ presents a Gaussian white noise, which meets

$$E[W(t)W(t + \tau)] = 2D\delta(\tau). \quad (2)$$

$D_C^\alpha X(t)$ in Equation (1) indicates the Caputo fractional derivative defined by

$$D_C^\alpha X(t) = \frac{1}{\Gamma(1 - \alpha)} \int_0^t \frac{\dot{X}(\mu)}{(t - \mu)^\alpha} d\mu, \quad (3)$$

in which $\Gamma(\cdot)$ denotes a gamma function. It should be noted that $D_C^\alpha X(t)$ in Equation (1) can be modeled as a damping force [36] and Stokes force [35].

In the absence of damping and forcing, the potential is given by

$$V(X) = \int_0^X g(\mu) d\mu. \quad (4)$$

Based on the procedure of stochastic averaging [26–30], one can take the following procedures:

$$X = X(t) = A \cos \Theta(t), \quad (5)$$

$$Y = \dot{X}(t) = -A\omega \sin \Theta(t), \quad (6)$$

$$\Theta(t) = \omega t + \Psi(t), \quad (7)$$

in which A , Θ and Ψ denote three random processes. $A(t)$ and $\Psi(t)$ indicate two slowly varying processes, while $\Theta(t)$ denotes a quickly varying process. Differentiating Equation (5) and equating the resulting equation to Equation (6), one could obtain

$$\dot{A} \cos \Theta - \dot{\Psi} A \sin \Theta = 0. \quad (8)$$

Differentiating Equation (6), using Equations (1), (5) and (6), one can also yield

$$\begin{aligned} & \dot{\Psi} \frac{g(A \cos \Theta)}{\omega} + \dot{A} \frac{g(A) - g(A \cos \Theta) \cos \Theta}{A\omega \sin \Theta} \\ & = \varepsilon c_1 D^\alpha(A \cos \Theta) + \varepsilon c_2 h(A \cos \Theta, -A\omega \sin \Theta) - W(t). \end{aligned} \quad (9)$$

Thus, \dot{A} and $\dot{\Psi}$ could be solved by Equations (8) and (9). Then, one yields

$$\frac{dA}{dt} = F_{11}(A, \Theta) + F_{12}(A, \Theta) + G_1(A, \Theta)W(t), \quad (10)$$

$$\frac{d\Psi}{dt} = F_2(A, \Theta) + G_2(A, \Theta)W(t), \quad (11)$$

where

$$F_1 = F_{11} + F_{12}, \quad (12)$$

$$F_{11} = \frac{A\omega \sin \Theta}{g(A)} c_1 D_C^\alpha(A \cos \Theta), \quad (13)$$

$$F_{12} = \frac{A\omega \sin \Theta}{g(A)} c_2 h(A \cos \Theta, -A\omega \sin \Theta), \quad (14)$$

$$F_2 = \frac{\omega \cos \Theta}{g(A)} c_1 D_C^\alpha(A \cos \Theta) + \frac{\omega \cos \Theta}{g(A)} c_2 h(A \cos \Theta, -A\omega \sin \Theta), \quad (15)$$

$$G_1 = -\frac{A\omega \sin \Theta}{g(A)}, \quad G_2 = -\frac{\omega \cos \Theta}{g(A)}. \quad (16)$$

Using Stratonovich–Khasminskii theorem [37], the averaged *Itô* equation of $A(t)$ is written as

$$dA = m(A)dt + \sigma(A)dB(t), \quad (17)$$

in which the drift coefficient and diffusion coefficient are given by

$$\begin{aligned} m(A) &= \varepsilon \left\langle F_{11} + F_{12} + D \frac{\partial G_1}{\partial A} G_1 + D \frac{\partial G_1}{\partial \Gamma} G_2 \right\rangle_{\Theta}, \\ \sigma^2(A) &= \varepsilon \left\langle 2DG_1^2 \right\rangle_{\Theta}, \end{aligned} \quad (18)$$

where averaging operation, $\langle \cdot \rangle_{\Theta}$, is given by

$$\langle \cdot \rangle_{\Theta} = \lim_{T \rightarrow \infty} \frac{1}{T} \int_0^T \langle \cdot \rangle dt = \frac{1}{2\pi} \int_0^{2\pi} \langle \cdot \rangle d\Theta. \tag{19}$$

Because A and Ψ vary slow with time, we can obtain

$$\Theta(\mu) = \Theta(t - s) = \Theta(t) - \omega s. \tag{20}$$

Using the definition of fractional calculus, the averaging term of Equation (18) could be derived by

$$\begin{aligned} \langle F_{11} \rangle_{\Theta} &= \left\langle \frac{A\omega \sin \Theta}{g(A)} c_1 D_C^\alpha (A \cos \Theta) \right\rangle_{\Theta} \\ &= \frac{c_1}{g(A)} \lim_{T \rightarrow \infty} \frac{1}{T} \int_0^T D_C^\alpha (A \cos \Theta) \times A\omega \sin \Theta dt \\ &= \frac{c_1}{\Gamma(1-\alpha)g(A)} \lim_{T \rightarrow \infty} \frac{1}{T} \int_0^T \left\{ \left[\int_0^t \frac{\dot{X}(\mu)}{(t-\mu)^\alpha} d\mu \right] \times A\omega \sin(\omega t + \Psi) \right\} dt \\ &= \frac{-c_1}{\Gamma(1-\alpha)g(A)} \lim_{T \rightarrow \infty} \frac{1}{T} \int_0^T \left\{ \left[\int_0^t \frac{A\omega \sin(\omega t + \Psi - \omega s)}{s^\alpha} ds \right] \times A\omega \sin(\omega t + \Psi) \right\} dt \\ &= \frac{-c_1 A^2 \omega^2}{\Gamma(1-\alpha)g(A)} \lim_{T \rightarrow \infty} \frac{1}{T} \left\{ \int_0^T \left[\int_0^t \frac{\cos(\omega s)}{s^\alpha} ds \right] \times \sin^2(\omega t + \Psi) \right\} dt \\ &\quad + \int_0^T \left\{ \left[\int_0^t \frac{\sin(\omega s)}{s^\alpha} ds \right] \times \cos(\omega t + \Psi) \sin(\omega t + \Psi) \right\} dt \triangleq M_1 + M_2. \end{aligned} \tag{21}$$

The first term in Equation (21) can be obtained

$$\begin{aligned} M_1 &= \frac{-c_1 A^2 \omega^2}{\Gamma(1-\alpha)g(A)} \lim_{T \rightarrow \infty} \frac{1}{T} \int_0^T \left[\int_0^t \frac{\cos(\omega s)}{s^\alpha} ds \right] d\left(\frac{2\omega t - \sin 2(\omega t + \Psi)}{4} \right) \\ &= \frac{-c_1 A^2 \omega^2}{4\Gamma(1-\alpha)g(A)} \left[\lim_{T \rightarrow \infty} \left(\frac{2\omega t - \sin 2(\omega t + \Psi)}{T} \right) \left(\int_0^t \frac{\cos(\omega s)}{s^\alpha} ds \right) \right]_0^T \\ &\quad + \lim_{T \rightarrow \infty} \frac{1}{T} \int_0^T \left(\int_0^t \frac{2\omega t - \sin 2(\omega t + \Psi)}{t^\alpha} \cos(\omega t) dt \right) \triangleq M_{11} + M_{12}. \end{aligned} \tag{22}$$

Before going on, the following two relations will be used,

$$\lim_{T \rightarrow \infty} \int_0^T \frac{\sin(\omega s)}{s^\alpha} ds = \omega^{\alpha-1} \Gamma(1-\alpha) \cos \frac{\alpha\pi}{2}, \tag{23}$$

$$\lim_{T \rightarrow \infty} \int_0^T \frac{\cos(\omega s)}{s^\alpha} ds = \omega^{\alpha-1} \Gamma(1-\alpha) \sin \frac{\alpha\pi}{2}. \tag{24}$$

Substituting Equations (23) and (24) into Equation (22), one has

$$\begin{aligned}
M_{11} &= \frac{-c_1 A^2 \omega^2}{4\Gamma(1-\alpha)g(A)} \lim_{T \rightarrow \infty} \left[2\omega^\alpha \Gamma(1-\alpha) \sin \frac{\alpha\pi}{2} - \frac{\sin 2(\omega t + \Psi) \omega^{\alpha-1} \Gamma(1-\alpha) \sin \frac{\alpha\pi}{2}}{T} \right] \\
&= \frac{-c_1 A^2}{2\Gamma(1-\alpha)g(A)} \omega^{\alpha+1} \Gamma(1-\alpha) \sin \frac{\alpha\pi}{2},
\end{aligned} \tag{25}$$

$$\begin{aligned}
M_{12} &= \frac{-c_1 A^2 \omega^2}{4\Gamma(1-\alpha)g(A)} \lim_{T \rightarrow \infty} \frac{1}{T} \int_0^T \frac{2\omega t - \sin 2(\omega t + \Psi)}{t^\alpha} \cos(\omega t) dt \\
&= \frac{-c_1 A^2 \omega^2}{4\Gamma(1-\alpha)g(A)} \left[\lim_{T \rightarrow \infty} \frac{1}{T} \int_0^T \frac{2\omega t \cos(\omega t)}{t^\alpha} dt - \lim_{T \rightarrow \infty} \frac{1}{T} \int_0^T \frac{\sin 2(\omega t + \Psi)}{t^\alpha} \cos(\omega t) dt \right] \\
&= 0,
\end{aligned} \tag{26}$$

$$\begin{aligned}
M_2 &= \frac{-c_1 A^2 \omega^2}{4g(A)\Gamma(1-\alpha)} \lim_{T \rightarrow \infty} \frac{1}{T} \int_0^T \left\{ \int_0^t \frac{\sin(\omega s)}{s^\alpha} ds \right\} \cos(\omega t + \Psi) \sin(\omega t + \Psi) dt \\
&= 0,
\end{aligned} \tag{27}$$

Thus,

$$\langle F_{11} \rangle_\Theta = M_{11} + M_{12} + M_2 = \frac{-c_1 A^2}{2g(A)} \omega^{\alpha+1} \sin \frac{\alpha\pi}{2}. \tag{28}$$

Therefore, the drift coefficient and diffusion coefficient in Equation (18) can be given by

$$\begin{aligned}
m(A) &= \varepsilon \langle F_{11} \rangle_\Theta + \frac{\varepsilon c_2 A}{2\pi g(A)} \int_0^{2\pi} \omega \sin \Theta h(A \cos \Theta, -A\omega \sin \Theta) d\Theta + \varepsilon D \left\langle \frac{\partial G_1}{\partial A} G_1 + \frac{\partial G_1}{\partial \Gamma} G_2 \right\rangle_\Theta, \\
\sigma^2(A) &= \varepsilon \langle 2DG_1^2 \rangle_\Theta.
\end{aligned} \tag{29}$$

FPKE associated with Equation (17) is given by

$$\frac{\partial p}{\partial t} = -\frac{\partial}{\partial A} [m(A)p] + \frac{1}{2} \frac{\partial^2}{\partial A^2} [\sigma^2(A)p]. \tag{30}$$

The boundary conditions for Equation (30) are

$$\begin{aligned}
p &= c, \quad A = 0; \\
P, \partial p / \partial A &\rightarrow 0, \quad A \rightarrow \infty.
\end{aligned} \tag{31}$$

Considering the boundary conditions in Equation (31), one can follow the normalization condition,

$$\int_0^\infty p(A) dA = 1. \tag{32}$$

The stationary solution of Equation (30) is given by

$$p(A) = \frac{C}{\sigma^2(A)} \exp \left[\int_0^A \frac{2m(u)}{\sigma^2(u)} du \right], \tag{33}$$

where C denotes a normalization constant given by

$$C = \left[\int_0^\infty \left(\frac{1}{\sigma^2(A)} \exp \left[\int_0^A \frac{2m(\mu)}{\sigma^2(\mu)} d\mu \right] \right) dA \right]^{-1}. \tag{34}$$

Thus, using Equation (33), the stationary PDF of Hamiltonian $H = V(A)$ can be given by

$$p(H) = p(A) \left| \frac{dA}{dH} \right| = \frac{p(A)}{g(A)} \Big|_{A=V^{-1}(H)}, \tag{35}$$

in which V^{-1} means the inverse function of H . Thus, the joint stationary PDF of the displacement and velocity could be given by

$$p(x, y) = \frac{p(H)}{T(H)} \Big|_{H=\frac{1}{2}y^2+V(x)}, \tag{36}$$

where

$$T(H) = \frac{2\pi}{\omega(A)} \Big|_{A=V^{-1}(H)}. \tag{37}$$

3. Two Fractional Order Stochastic Morse Oscillators

3.1. Fractional Order Stochastic Morse Oscillator with Constant Damping

In this subsection, we will consider a Caputo fractional damping stochastic Morse oscillator with Gaussian white noise given by

$$\ddot{X}(t) + b_1 D_C^\alpha X(t) + b_2 X\dot{X} + \beta(e^{-X} - e^{-2X}) = W(t). \tag{38}$$

in which $W(t)$ presents a zero mean Gaussian white noise meeting Equation (2), b_1 denotes damping coefficient, b_2 and β are constant coefficients. Based on the results in Section 2, the following transformations are adopted:

$$\begin{aligned} X &= X(t) = A \cos \Phi(t), \\ Y &= \dot{X}(t) = -A\omega \sin \Phi(t), \\ \Phi(t) &= \omega t + \Gamma, \\ V(X) &= \frac{1}{2}\beta e^{-X}(e^{-X} - 2). \end{aligned} \tag{39}$$

Using transformation (39), from Equation (38), one can follow two parts,

$$\frac{dA}{dt} = \varepsilon F_{11}(A, \Theta) + \varepsilon F_{12}(A, \Theta) + G_1(A, \Theta)W(t), \tag{40}$$

$$\frac{d\Gamma}{dt} = \varepsilon F_2(A, \Theta) + G_2(A, \Theta)W(t). \tag{41}$$

where

$$\begin{aligned} h_{11}(A, \Gamma) &= \frac{b_1}{\omega} \sin \Phi D_C^\alpha (A \cos \Phi), \\ h_{12}(A, \Gamma) &= -b_2 A^2 \sin^2 \Phi \cos \Phi + \frac{\beta}{\omega} \sin \Phi (e^{-A \cos \Phi} - e^{-2A \cos \Phi}) - A\omega \sin \Phi \cos \Phi, \\ h_{21}(A, \Gamma) &= -\frac{b_1}{\omega A} \cos \Phi D_C^\alpha (A \cos \Phi), \\ h_{22}(A, \Gamma) &= b_2 A \cos^2 \Phi \sin \Phi + \frac{\beta}{\omega A} \cos \Phi (e^{-A \cos \Phi} - e^{-2A \cos \Phi}) - \omega \cos^2 \Phi, \\ g_1(A, \Gamma) &= -\frac{\sin \Phi}{\omega}, g_2(A, \Gamma) = -\frac{\cos \Phi}{\omega A}. \end{aligned} \tag{42}$$

Utilizing the procedure in the Section 2, $It\hat{o}$ differential Equation (17) with the drift coefficient and diffusion coefficient given by

$$\begin{aligned} m(A) &= -\frac{Ab_1}{2}\omega^{\alpha-1} \sin \frac{\alpha\pi}{2} + \frac{D}{2\omega^2 A}, \\ \sigma^2(A) &= \frac{D}{\omega^2}. \end{aligned} \tag{43}$$

Thus, stationary PDF of the system (38) could be given by

$$p(A) = \frac{b_1 A \omega^{\alpha+1} \sin \frac{\alpha\pi}{2}}{D} \exp\left(-\frac{b_1 \omega^{\alpha+1} \sin \frac{\alpha\pi}{2} A^2}{2D}\right). \quad (44)$$

From Equations (33) and (35), the joint stationary PDF of X and Y could be written as

$$p_{st}(X, Y) = \frac{b_1 \omega^{\alpha+2} \sin \frac{\alpha\pi}{2}}{2\pi D} \exp\left[-\frac{b_1 \omega^{\alpha+1} \sin \frac{\alpha\pi}{2}}{2D} \left(X^2 + \frac{Y^2}{\omega^2}\right)\right]. \quad (45)$$

Correspondingly, stationary PDF of displacement and stationary PDF of velocity could be, respectively, obtained as follows:

$$p_{st}(X) = \frac{b_1 \omega^{\alpha+3} \sqrt{\pi} \sin \frac{\alpha\pi}{2}}{2\pi D \sqrt{\frac{b_1 \omega^{\alpha+1} \sin \frac{\alpha\pi}{2}}{2D}}} \exp\left[-\frac{b_1 \omega^{\alpha+1} \sin \frac{\alpha\pi}{2}}{2D} X^2\right], \quad (46)$$

$$p_{st}(Y) = \frac{b_1 \omega^{\alpha+2} \sqrt{\pi} \sin \frac{\alpha\pi}{2}}{2\pi D \sqrt{\frac{b_1 \omega^{\alpha+1} \sin \frac{\alpha\pi}{2}}{2D}}} \exp\left[-\frac{b_1 \omega^{\alpha+1} \sin \frac{\alpha\pi}{2}}{2\omega^2 D} Y^2\right]. \quad (47)$$

The stationary PDF versus displacement for a different fractional derivative order is plotted in Figure 1. To testify the precision of the analytical results, one can apply the stochastic Euler method (Equation (A1) in the Appendix A), and the results of Monte Carlo simulation for system (38) are also demonstrated in Figure 1.

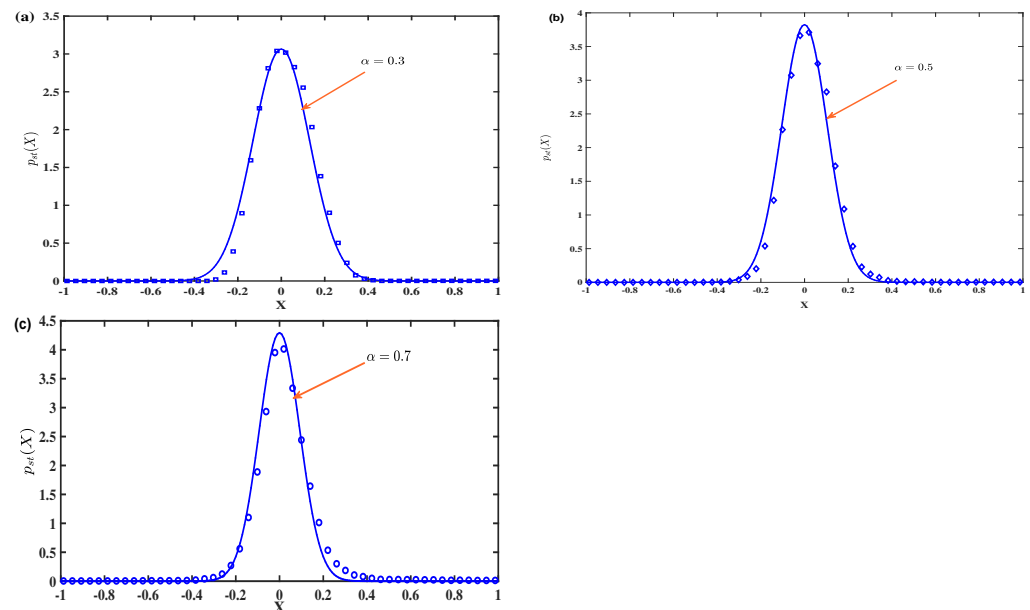


Figure 1. Stationary PDF of displacement X of system (38) for $b_1 = 0.13, D = 0.001, \omega = 1.0$. — signifies analysis results, while \circ represents numerical simulation results. (a) $\alpha = 0.3$; (b) $\alpha = 0.5$; (c) $\alpha = 0.7$.

It can be observed, from Figure 1, that the analytical results using the stochastic averaging procedure coincide with numerical simulation of a stochastic Morse oscillator (38). Meanwhile, it can be concluded that fractional order α greatly impacts PDF of stochastic Morse oscillator (38). Under the same noise intensity, the higher fractional order results in PDF lifting while the peak of PDF declines with the decline of fractional order α . The stationary PDF versus displacement for different noise intensities D is plotted in Figure 2. One can figure out that the peak of PDF decreases with the rise of noise intensity D .

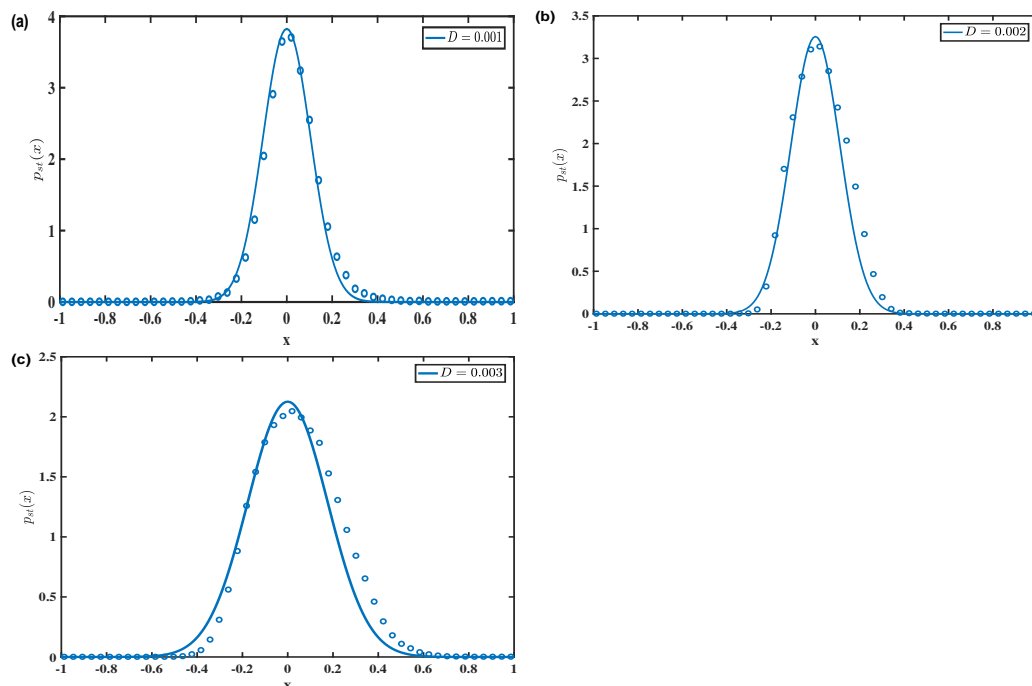


Figure 2. Stationary PDF of amplitude A of system (38) for $b_1 = 0.13, \alpha = 0.5, \omega = 1.0$. — signifies analysis results, while \circ represents numerical simulation results. (a) $D = 0.001$; (b) $D = 0.002$; (c) $D = 0.001$.

The stationary PDF versus amplitude for different b_1 is plotted in Figure 3. One can find that the peak of PDF lifts with the rising of b_1 . Figure 4 displays the stationary PDF versus amplitude for different ω . One can see that the peak of PDF lifts with the rising of ω . Thus, both b_1 and ω can lift the response of PDF.

Figure 5 exhibits the stationary joint PDF of displacement and velocity, respectively, derived by using procedure of stochastic averaging and by using numerical simulation of system (49) with $\alpha = 0.3$. It can be found out that the analysis results of PDF agree with the PDF of numerical simulation.

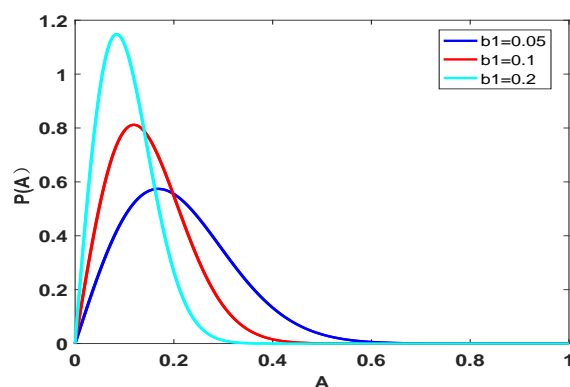


Figure 3. Stationary PDF of system (38) versus amplitude A with $D = 0.001, \alpha = 0.5, \omega = 1.0$.

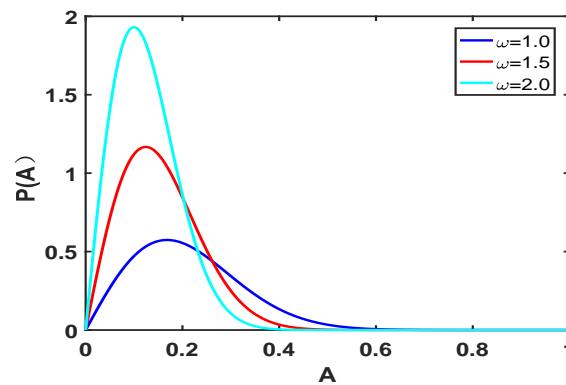


Figure 4. Stationary PDF of system (38) versus amplitude A with $b_1 = 0.05$, $D = 0.001$, $\alpha = 0.5$.

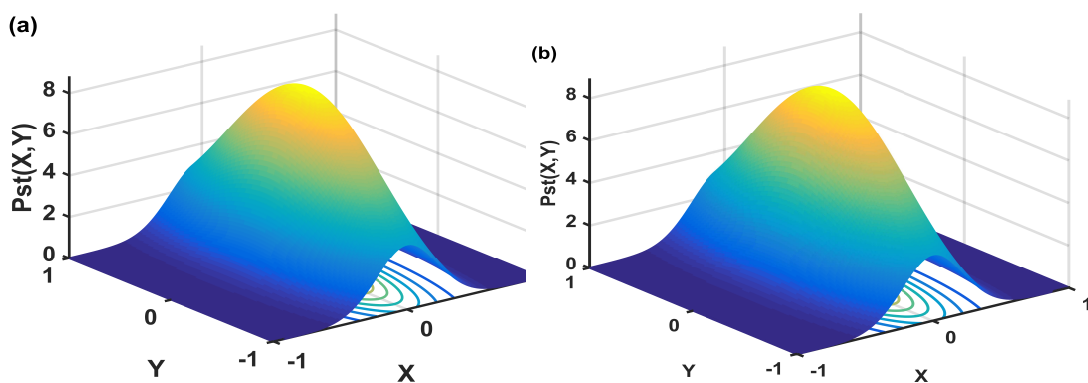


Figure 5. Stationary joint PDF of system (38) versus displacement and velocity with $b_1 = 0.05$, $D = 0.01$, $\omega = 3.0$. (a) Analysis results; (b) numerical simulation results.

3.2. Fractional Order Stochastic Morse Oscillator with Nonlinear Damping

In this subsection, we will focus on a fractional order stochastic Morse oscillator with nonlinear damping subjected to a Gaussian white noise given by

$$\ddot{X} + (a_1X^4 - a_2X^2 + a_0)D_C^\alpha X + (b_1 + b_2X^2)\dot{X} + \beta(e^{-X} - e^{-2X}) = W(t). \tag{48}$$

in which $W(t)$ presents a zero mean Gaussian white noise meeting Equation (2). $a_1X^4 - a_2X^2 + a_0$ denotes a nonlinear damping function, where a_1, a_2, a_0 in Equation (48) are constant coefficients. b_1, b_2 are constant coefficients.

Using the procedure in Section 2, Itô differential Equation (17) with the drift coefficient and diffusion coefficient written as

$$\begin{aligned} m(A) &= \left(-\frac{a_1A^5}{16} + \frac{a_2A^3}{8} - \frac{a_0A}{2}\right)\omega^{\alpha-1} \sin \frac{\alpha\pi}{2} - \left(\frac{b_1A}{2} + \frac{b_2A^3}{8}\right) + \frac{D}{2\omega^2A}, \\ \sigma(A) &= \frac{D}{\omega^2}. \end{aligned} \tag{49}$$

Thus, one can easily derive the stationary PDF of the system (48) given by

$$p(A) = \frac{C\omega^2A}{D} \exp\left[\frac{\omega^{\alpha+1} \sin \frac{\alpha\pi}{2}}{D} \left(-\frac{a_1}{48}A^6 + \frac{a_2}{16}A^4 - \frac{a_0}{2}A^2\right) - \frac{b_1\omega^2}{2D}A^2 - \frac{b_2\omega^2}{16D}A^4\right], \tag{50}$$

in which C denotes a normalization constant.

Stochastic P-bifurcation is related to the peak number of the steady-state PDF curve. Stochastic P-bifurcation occurs with the variation of peak number of the stationary PDF curve. For convenience, one can record $p(A)$ as

$$p(A) = C_1R(A, D, \omega, \alpha, a_0, a_1, a_2, b_1, b_2) \exp(A, D, \omega, \alpha, a_0, a_1, a_2, b_1, b_2). \tag{51}$$

Based on singularity theory [38], the stationary PDF satisfies the conditions given by

$$\frac{\partial p(A)}{\partial A} = 0, \frac{\partial^2 p(A)}{\partial A^2} = 0. \quad (52)$$

From Equations (50)–(52), one can obtain the critical condition of P-bifurcation for system (48) with noise density D and fractional order α

$$a_1 \omega^{\alpha-1} \sin \frac{\alpha\pi}{2} A^6 - 2(a_2 \omega^{\alpha-1} \sin \frac{\alpha\pi}{2} - b_2) A^4 + 8(a_0 \omega^{\alpha-1} \sin \frac{\alpha\pi}{2} + b_1) A^2 - \frac{8D}{\omega^2} = 0, \quad (53)$$

where amplitude A satisfies:

$$3a_1 \omega^{\alpha-1} \sin \frac{\alpha\pi}{2} A^4 - 4(a_2 \omega^{\alpha-1} \sin \frac{\alpha\pi}{2} - b_2) A^2 + 8(a_0 \omega^{\alpha-1} \sin \frac{\alpha\pi}{2} + b_1) = 0. \quad (54)$$

In order to address stochastic P-bifurcation with fractional order α and noise density D , for convenience, one can take $\omega = 2$, $a_0 = 0.12$, $a_1 = 1$, $a_2 = 1$, $b_1 = 0.05$, $b_2 = 0.05$. Figure 6 exhibits P-bifurcation diagram, (α, D) plane, which was obtained from Equations (53) and (54). In Figure 6a,c, the solid line L_1 is the critical curve dividing the parameter plane into domain B_1 , domain B_2 and B_3 . Figure 6b exhibits PDF for three sets of parameters. For instance, in Figure 6a, in (α, D) plane, one can take the first point $(0.25, 0.01) \in B_1$, the second point $(0.55, 0.01) \in B_2$, and the third point $(0.75, 0.01) \in B_3$. The corresponding stationary PDF for each parameter point is plotted in Figure 6b. From Figure 6b, it can be discovered that the stationary PDF curve is unimodal in domain B_1 , while the stationary PDF is bimodal in domain B_2 , and the stationary PDF is unimodal in domain B_3 . Figure 6b implies that stationary PDF shifts from a single peak to double peaks with the rise of α from 0.25 to 0.55. The variation of peak number in the stationary PDF reveals the occurrence of stochastic P-bifurcation. Additionally, in Figure 6c, one can take $\alpha = 0.55$, and take D as 0.001, 0.006. The corresponding stationary PDF for each parameter point is shown in Figure 6d, which reveals the variation of the peak number in PDF. With the rise of noise intensity D from 0.001 to 0.006, PDF varies from a single peak to double peaks. Apparently, stochastic P-bifurcation occurs.

Figure 7 plots a P-bifurcation diagram, (ω, D) plane, which was obtained from Equations (53) and (54). Here, the other parameters are taken as $\alpha = 0.55$, $a_0 = 0.12$, $a_1 = 1$, $a_2 = 1$, $b_1 = 0.05$, $b_2 = 0.05$. The solid line L in Figure 7a,c divides the (ω, D) plane into domain S_1 and domain S_2 . Similarly, one can take one point $(1.5, 0.004) \in S_1$ and another point $(1.5, 0.007) \in S_2$, and the corresponding stationary PDF for each parameter point is demonstrated in Figure 7b. From Figure 7b, one can discover the stationary PDF curve is unimodal in domain S_2 , while the stationary PDF is bimodal in domain S_1 . This phenomenon implies the stationary PDF shifts from single peak to double peak as D decreases from 0.007 to 0.004. The variation of peak number of the stationary PDF also reveals the occurrence of P-bifurcation. Additionally, in Figure 7c, one can take $D = 0.004$ and take ω as 0.5, 1.5, 2.5. The corresponding stationary PDF for each parameter point is shown in Figure 7d, which reveals the variation of the peak number in PDF. Obviously, stochastic P-bifurcation occurs.

Figure 8 demonstrates a P-bifurcation diagram, (b_1, D) plane, which was obtained from Equations (53) and (54). Here, one can take $\alpha = 0.5$, $a_0 = 0.12$, $a_1 = 1$, $a_2 = 1$, $b_2 = 0.05$. The solid line L in Figure 8a,c divides the (b_1, D) plane into domain C_1 and domain C_2 . The PDFs for three set of parameters are plotted in Figure 8b. Similarly, take points $(0.02, 0.01) \in C_2$, $(0.04, 0.01) \in C_1$ and $(0.06, 0.01) \in C_2$, and we obtain the corresponding stationary PDF for each parameter point. One can figure out from Figure 8b that the stationary PDF curve is unimodal in domain C_2 , while the stationary PDF is bimodal in domain C_1 . For $b_1 = 0.02$, $b_1 = 0.04$, and $b_1 = 0.06$, one can find that the stationary PDF shifts from a single peak to double peaks, and then PDF eventually turns to a single peak. The variation of the peak number in the stationary PDF reveals the occurrence of P-bifurcation. Additionally, one can take $b_1 = 0.045$ and take D as

0.015, 0.025. The corresponding stationary PDF for each parameter point is depicted in Figure 8d, which exhibits the variation of the peak number in PDF. Apparently, stochastic P-bifurcation occurs.

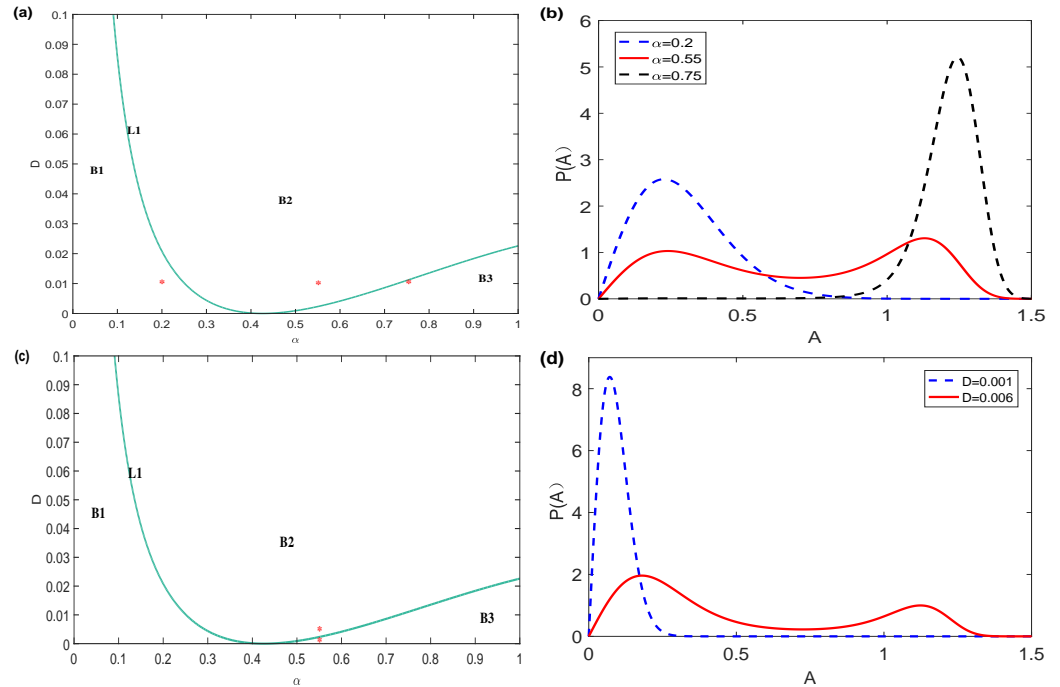


Figure 6. P-bifurcation with $\omega = 2, a_0 = 0.12, a_1 = 1, a_2 = 1, b_1 = 0.05, b_2 = 0.05$. (a) P-bifurcation diagram, (α, D) plane, with three marked points. (b) PDF versus amplitude A for various α with $D = 0.01$. (c) P-bifurcation diagram, (α, D) plane, with two marked points. (d) PDF versus amplitude A for various D with $\alpha = 0.55$.

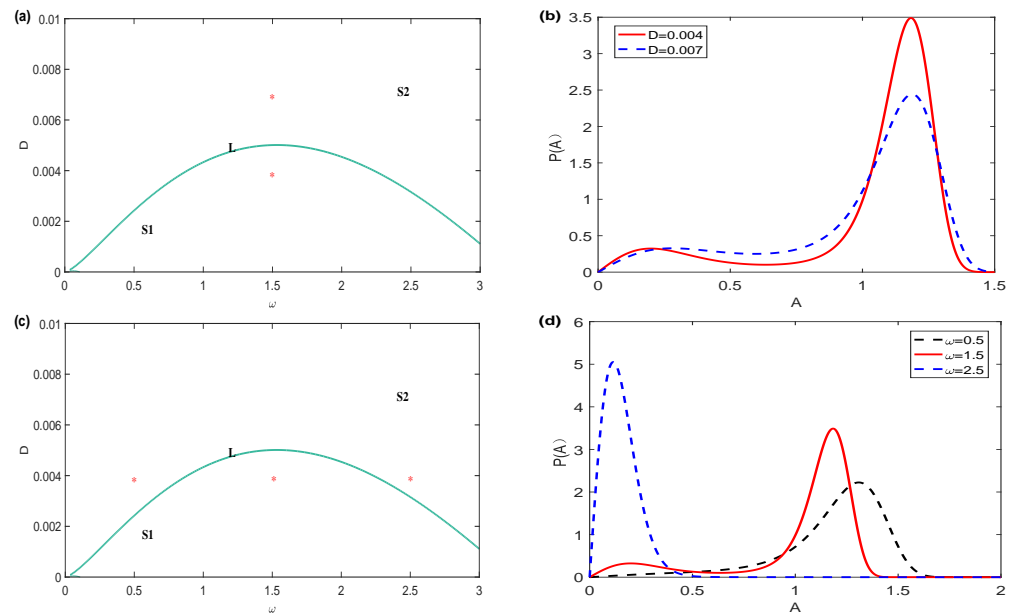


Figure 7. P-bifurcation with $\alpha = 0.55, a_0 = 0.12, a_1 = 1, a_2 = 1, b_1 = 0.05, b_2 = 0.05$. (a) P-bifurcation, (ω, D) plane, with two marked points. (b) PDF versus amplitude A for various D with $\omega = 1.5$. (c) P-bifurcation, (ω, D) plane, with three marked points. (d) PDF versus amplitude A for various ω with $D = 0.004$.

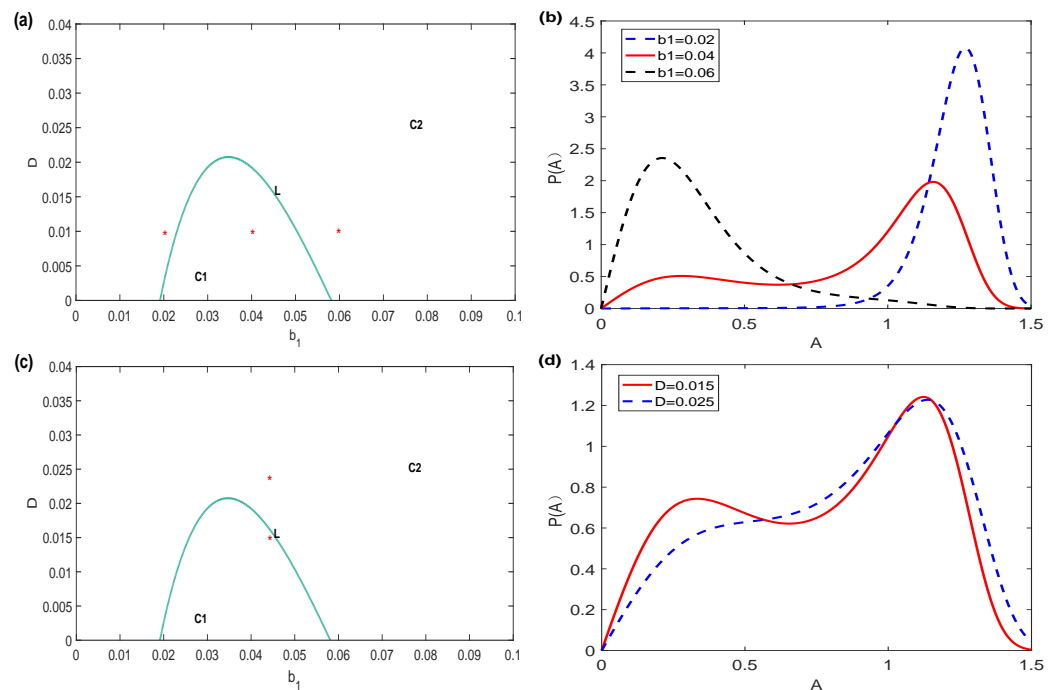


Figure 8. P-bifurcation with $\alpha = 0.5$, $a_0 = 0.12$, $a_1 = 1$, $a_2 = 1$, $b_2 = 0.05$. (a) P-bifurcation, (b_1, D) plane, with three marked points. (b) PDF versus amplitude A for various b_1 with $D = 0.01$. (c) P-bifurcation, (b_1, D) plane, with two marked points. (d) PDF versus amplitude A for various D with $b_1 = 0.045$.

4. Conclusions

Due to the application of stochastic analysis, this work focuses on the approximate solution of a fractional damping stochastic nonlinear equation with Gaussian white noise. To begin with, the analytic solution of a stochastic nonlinear equation is derived by the procedure of stochastic averaging. Moreover, FPKE associated with the $It\hat{o}$ equation has been obtained. Correspondingly, the analytic expression of stationary PDF of a fractional damping stochastic nonlinear equation has been derived. Considering the description of the diatomic molecule in electromagnetic fields, the stochastic analyses of two fractional order stochastic Morse oscillators have been addressed. One can figure out that the stationary PDF of a Morse oscillator versus the displacement amplitude and velocity obtained by using the stochastic averaging method identified with simulation results. Furthermore, the critical condition of stochastic P-bifurcation has been derived. Stochastic P-bifurcations are explored via the critical condition. Additionally, P-bifurcation diagrams, (α, D) plane, (ω, D) plane and (b_1, D) plane have been addressed in detail. We conclude that the P-bifurcation behavior of the fractional order stochastic Morse oscillator with nonlinear damping could be caused by α, D, ω and b_1 .

Author Contributions: Conceptualization, G.H.; Software, Y.T. and Y.P.; Formal analysis, G.H.; Investigation, Y.T., Y.P., W.L. and W.Z.; Resources, W.L.; Writing—original draft, Y.T.; Writing—review & editing, W.Z.; Supervision, G.H.; Funding acquisition, G.H. All authors have read and agreed to the published version of the manuscript

Funding: This work was supported by the National Natural Science Foundation of China (No. 11601450, 11961006, 11526172), Guangxi Natural Science Foundation (No. 2020GXNSFAA159100, AD21159013, 2021GXNSFAA220033), Natural Science Foundation of Guangxi Minzu University (No. 2019KJQD02), Xiangsi Lake Young Scholars Innovation Team of Guangxi Minzu University (No. 2021RSCXSHQN05), and Sichuan Youth Science Project (No. 2022NSFSC1840).

Data Availability Statement: Not applicable.

Conflicts of Interest: The authors declare no conflict of interest.

Appendix A. Numerical Simulation

A numerical simulation of Equation (38) is used by the stochastic Euler method given by the following approximation:

$$x(t_n) = \frac{2x(t_{n-1}) - x(t_{n-2}) - b_1 \Delta t^{2-\alpha} \sum_{j=1}^{n-1} (-1)^j \binom{\alpha}{j} x(t_{n-j}) + b_2 x(t_{n-1}) \Delta t x(t_{n-2})}{1 + b_2 x(t_{n-1}) \Delta t + b_1 \Delta t^{2-\alpha}} + \frac{-\Delta t^2 \beta \{\exp[-x(t_{n-1})] - \exp[-2x(t_{n-1})]\} + \Delta t^2 W(t_{n-1})}{1 + b_2 x(t_{n-1}) \Delta t + b_1 \Delta t^{2-\alpha}}, \quad (\text{A1})$$

$$\text{where } \binom{\alpha}{j} = \frac{\alpha(\alpha-1)(\alpha-2)\dots(\alpha-j+1)}{j!}.$$

References

1. Oldham, K.B. Fractional differential equations in electrochemistry. *Adv. Eng. Softw.* **2010**, *41*, 9–12. [CrossRef]
2. Khan, I.; Abrob, K.A.; Mirbharb, M.N.; Tlili, I. Thermal analysis in Stokes' second problem of nanofluid: Applications in thermal engineering. *Case Stud. Therm. Eng.* **2018**, *12*, 271–275. [CrossRef]
3. Riewe, F. Mechanics with fractional derivatives. *Phys. Rev. E* **1997**, *55*, 3581. [CrossRef]
4. Mbodje, B.; Montseny, G. Boundary fractional derivative control of the wave equation. *IEEE Trans. Autom. Control* **1995**, *40*, 378–382. [CrossRef]
5. Rogers, L. Operators and fractional derivatives for viscoelastic constitutive equations. *J. Rheol.* **1983**, *27*, 351–372. [CrossRef]
6. Heymans, N.; Bauwens, J.C. Fractal rheological models and fractional differential equations for viscoelastic behavior. *Rheol. Acta* **1994**, *33*, 210–219. [CrossRef]
7. Hilfer, R. *Applications of Fractional Calculus in Physics*; World Scientific: Singapore, 2000.
8. Anderson, D.R.; Ulness, D.J. Properties of the Katugampola fractional derivative with potential application in quantum mechanics. *J. Math. Phys.* **2015**, *56*, 063502. [CrossRef]
9. Bagley, R.L.; Torvik, P.J. A theoretical basis for the application of fractional calculus to viscoelasticity. *J. Rheol.* **1983**, *27*, 201–210. [CrossRef]
10. Qiu, L.; He, G.; Peng, Y.; Cheng, H.; Tang, Y. Noise Spectral of GML Noise and GSR Behaviors for FGLE with Random Mass and Random Frequency. *Fractal Fract.* **2023**, *7*, 177. [CrossRef]
11. Cajo, R.; Zhao, S.; Birs, I.; Espinoza, V.; Fernández, E.; Plaza, D.; Salcan-Reyes, G. An Advanced Fractional Order Method for Temperature Control. *Fractal Fract.* **2023**, *7*, 172. [CrossRef]
12. Assadi, I.; Charef, A.; Copot, D.; De Keyser, R.; Bensouici, T.; Ionescu, C. Evaluation of respiratory properties by means of fractional order models. *Biomed. Signal Process. Control* **2017**, *34*, 206–213. [CrossRef]
13. Khandekar, D.C.; Bhagwat, D.K.S.L.K.; Lawande, S.V.; Bhagwat, K.V. *Path Integral Methods and Their Applications*; Allied Publishers: New Delhi, India, 2002.
14. Suarez, L.E.; Shokooh, A. An eigenvector expansion method for the solution of motion containing fractional derivatives. *J. Appl. Mech.* **1997**, *64*, 629–635. [CrossRef]
15. Rossikhin, Y.A.; Shitikova, M.V. Analysis of free non-linear vibrations of a viscoelastic plate under the conditions of different internal resonances. *Int. J. Non-Linear Mech.* **2006**, *41*, 313–325. [CrossRef]
16. Li, J.; Zhang, J.; Ge, W.; Liu, X. Multi-scale methodology for complex systems. *Chem. Eng. Sci.* **2004**, *59*, 1687–1700. [CrossRef]
17. Podlubny, I. The Laplace transform method for linear differential equations of the fractional order. *arXiv* **1997**, arXiv:funct-an/9710005.
18. Singh, K.; Saxena, R.; Kumar, S. Caputo-based fractional derivative in fractional Fourier transform domain. *IEEE J. Emerg. Sel. Top. Circuits Syst.* **2013**, *3*, 330–337. [CrossRef]
19. Gaul, L.; Klein, P.; Kempfle, S. Impulse response function of an oscillator with fractional derivative in damping description. *Mech. Res. Commun.* **1989**, *16*, 297–305. [CrossRef]
20. Gliklikh, Y.E. *Global and Stochastic Analysis with Applications to Mathematical Physics*; Springer: Berlin/Heidelberg, Germany, 2011.
21. Roberts, J.B.; Spanos, P.D. Stochastic averaging: An approximate method of solving random vibration problems. *Int. J. Non-Linear Mech.* **1986**, *21*, 111–134. [CrossRef]
22. Huang, Z.L.; Jin, X.L. Response and stability of a SDOF strongly nonlinear stochastic system with light damping modeled by a fractional derivative. *J. Sound Vib.* **2009**, *319*, 1121–1135. [CrossRef]
23. Yang, Y.; Xu, W.; Jia, W.; Han, Q. Stationary response of nonlinear system with Caputo-type fractional derivative damping under Gaussian white noise excitation. *Nonlinear Dyn.* **2015**, *79*, 139–146. [CrossRef]
24. Jin, C.; Sun, Z.; Xu, W. A novel stochastic bifurcation and its discrimination. *Commun. Nonlinear Sci. Numer. Simul.* **2022**, *110*, 106364. [CrossRef]

25. Horsthemke, W. *Noise Induced Transitions: Non-Equilibrium Dynamics in Chemical Systems*; Springer: Berlin/Heidelberg, Germany, 1984; pp. 150–160.
26. Zhu, W.Q.; Huang, Z.L. Stochastic Hopf bifurcation of quasi-nonintegrable-Hamiltonian systems. *Int. J. Non-Linear Mech.* **1999**, *34*, 437–447. [[CrossRef](#)]
27. Yang, Y.G.; Sun, Y.H.; Xu, W. Bifurcation Analysis of an Energy Harvesting System with Fractional Order Damping Driven by Colored Noise. *Int. J. Bifurc. Chaos* **2021**, *31*, 2150223. [[CrossRef](#)]
28. Schenk-Hoppé, K.R. Bifurcation scenarios of the noisy Duffing-van der Pol oscillator. *Nonlinear Dyn.* **1996**, *11*, 255–274. [[CrossRef](#)]
29. Schenk-Hoppé, K.R. Stochastic Hopf bifurcation: An example. *Int. J. Non-Linear Mech.* **1996**, *31*, 685–692. [[CrossRef](#)]
30. Zhu, W.Q.; Huang, Z.L. Lyapunov exponents and stochastic stability of quasi-integrable-Hamiltonian systems. *J. Appl. Mech.* **1999**, *66*, 211–217. [[CrossRef](#)]
31. Beigie, D.; Wiggins, S. Dynamics associated with a quasiperiodically forced Morse oscillator: Application to molecular dissociation. *Phys. Rev. A* **1992**, *45*, 4803. [[CrossRef](#)]
32. Knop, W.; Lauterborn, W. Bifurcation structure of the classical Morse oscillator. *J. Chem. Phys.* **1990**, *93*, 3950–3957. [[CrossRef](#)]
33. Chatterjee, S.; Sekh, G. A.; Talukdar, B. Fisher information for the Morse oscillator. *Rep. Math. Phys.* **2020**, *85*, 281–291. [[CrossRef](#)]
34. Abirami, K.; Rajasekar, S.; Sanjuan, M.A.F. Vibrational resonance in the Morse oscillator. *Pramana* **2013**, *81*, 127–141. [[CrossRef](#)]
35. Rossikhin, Y.A.; Shitikova, M.V. Application of fractional derivatives to the analysis of damped vibrations of viscoelastic single mass systems. *Acta Mech.* **1997**, *120*, 109–125. [[CrossRef](#)]
36. Shen, Y.; Yang, S.; Sui, C. Analysis on limit cycle of fractional-order van der Pol oscillator. *Chaos Solitons Fractals* **2014**, *67*, 94–102. [[CrossRef](#)]
37. Khasminskij, R.Z. On the principle of averaging the Itov's stochastic differential equations. *Kybernetika* **1968**, *4*, 260–279.
38. Golubitsky, M.; Schaeffer, D. *A Theory for Imperfect Bifurcation via Singularity Theory*; Wisconsin Univ-Madison Mathematics Research Center: Madison, WI, USA, 1978.

Disclaimer/Publisher's Note: The statements, opinions and data contained in all publications are solely those of the individual author(s) and contributor(s) and not of MDPI and/or the editor(s). MDPI and/or the editor(s) disclaim responsibility for any injury to people or property resulting from any ideas, methods, instructions or products referred to in the content.